Experimental Physiology

Strain softening behaviour in nonviable rat right-ventricular trabeculae in the presence and the absence of butanedione monoxime

R. S. Kirton[1,3], A. J. Taberner[1,5], P. M. F. Nielsen[1,3], A. A. Young[1,2,4] and D. S. Loiselle[1,4]

[1]*Bioengineering Institute, and Departments of* [2]*Anatomy,* [3]*Engineering Science and* [4]*Physiology, The University of Auckland, Auckland, New Zealand*
[5]*Department of Mechanical Engineering, Massachusetts Institute of Technology, Cambridge, MA, USA*

Strain softening is commonly reported during mechanical testing of passive whole hearts. It is typically manifested as a stiffer force–extension relationship in the first deformation cycle relative to subsequent cycles and is distinguished from viscoelasticity by a lack of recovery of stiffness, even after several hours of rest. The cause of this behaviour is presently unknown. In order to investigate its origins, we have subjected trabeculae to physiologically realistic extensions (5–15% of muscle length at 26°C and 0.5 mM Ca^{2+}), while measuring passive force and dynamic stiffness. While we did not observe strain softening in viable trabeculae, we found that it was readily apparent in nonviable (electrically inexcitable) trabeculae undergoing the same extensions. This result was obtained in both the presence and absence of 2,3-butanedione monoxime (BDM). Furthermore, BDM had no effect on the passive compliance of viable specimens, while its presence partly inhibited, but could not prevent, stiffening of nonviable specimens. Loss of viability was accompanied by a uniform increase of dynamic stiffness over all frequencies examined (0.2–100 Hz). The presence of strain softening during length extensions of nonviable tissue resulted in a comparable uniform decrease of dynamic stiffness. It is therefore concluded that strain softening is neither intrinsic to viable rat right ventricular trabeculae nor influenced by BDM but, rather, reflects irreversible damage of tissue in partial, or full, rigor.

(Received 9 March 2004; accepted after revision 29 June 2004; first published online 15 July 2004)
Corresponding author R. S. Kirton: Bioengineering Institute, The University of Auckland, 70 Symonds Street, Auckland, New Zealand. Email: r.kirton@auckland.ac.nz

The diastolic mechanical properties of cardiac muscle are important determinants of cardiac function, with excessive myocardial passive stiffness contributing to diastolic heart failure (Gutierrez & Blanchard, 2004). In order to characterize these properties, it is necessary to determine the passive pressure–volume relationship of the heart. While this would seem at first glance to be a trivial experimental exercise, closer scrutiny reveals unavoidable difficulties. These arise from the presence of the coronary circulation. For if the myocardial tissues are perfused while inflating a cardiac chamber, then the presence of incompressible fluid in a vascular compartment of variable volume that is embedded within the tissue inevitably distorts the pressure response to a change of volume (Fiegl, 1983; McCulloch *et al.* 1992). In consequence, unambiguous interpretation of results is precluded. This problem can be obviated by making passive pressure–volume measurements in the absence of fluid in the coronary circulation, i.e. by resorting to the use of nonperfused tissue. The risk of this approach, of course, is induction of ischaemia-induced damage to myocardial tissues whose basal metabolic rate continues in the absence of coronary perfusion.

Under such ischaemic conditions, strain softening is commonly observed during physiological levels of strain in both whole hearts and small tissue blocks (Emery *et al.* 1997, 1998; Dokos *et al.* 2002). Strain softening is manifest as a stiffer stress–strain relationship on the first loading cycle than in all subsequent cycles. Unlike viscoelastic relaxation, the tissue does not recover, even after hours of rest. As with whole hearts and tissue blocks, biaxial extension of canine myocardial slices required preconditioning stretches of the samples, which were larger than, or equal to, the magnitude of the stretches

 DOI: 10.1113/expphysiol.2004.027623

used to determine tissue properties (Humphrey *et al.* 1990). This preconditioning was required to ensure that the specimen was 'stress free'.

To gain an understanding of strain softening in whole hearts and tissue blocks, its mechanisms in smaller, simpler cardiac preparations, such as trabeculae, must first be understood. We (Kirton *et al.* 2004) have recently shown an absence of strain softening during passive axial extension of superfused, viable (i.e. electrically responsive), right ventricular (RV) rat trabeculae. This absence of strain softening was independent of the presence of 2,3-butanedione monoxime (BDM).

One possible cause of the appearance of strain softening behaviour is tissue ischaemia. Many studies have applied ischaemic or hypoxic interventions to cardiac preparations, ranging from whole heart studies to isolated myocytes, to investigate the mechanisms responsible for heart failure during ischaemia. Studies of hypoxia in cardiac trabeculae and papillary muscles have demonstrated loss of response to stimulation, increase of high-frequency stiffness and increase in contracture force (Leijendekker *et al.* 1990; Bucx, 1993; Hajjar *et al.* 1994). Although there is some controversy, most studies report that ischaemic or hypoxic episodes in cardiac tissue cause depletion of ATP, consequently leading to rigor cross-bridge formation and tissue contracture (Stern *et al.* 1985; Haworth *et al.* 1988; Koretsune & Marban, 1990). The progress of rigor cross-bridge formation has been monitored by changes in trabecula stiffness, as determined by small (∼1% of muscle length) sinusoidal muscle length perturbations at 1 and 100 Hz (Leijendekker *et al.* 1990; Bucx, 1993).

In order to investigate these effects, we examined the stress–strain behaviour of trabeculae that had become nonviable (i.e. electrically nonresponsive) either spontaneously (i.e. in the course of a lengthy experiment) or intentionally (i.e. by experimental withdrawal of oxygen). Furthermore, because of the putative role of BDM in preventing cross-bridge formation, we have examined its ability to prevent strain softening in both the presence and absence of oxygen.

The objectives of the present study were therefore to compare stress–strain relationships and muscle stiffness of viable trabeculae, of spontaneously nonviable (i.e. unresponsive to electrical stimulation) trabeculae, and of previously viable trabeculae that had been rendered hypoxic. The following questions were addressed. (i) Do methods that have shown no evidence of strain softening in viable trabeculae (Kirton *et al.* 2004) reveal strain softening in nonviable specimens? (ii) Is strain softening behaviour observed in hypoxic trabeculae? (iii) Are the stress–strain relationships observed in spontaneously nonviable trabeculae similar to those seen in hypoxic trabeculae? (iv) What are the effects of BDM on strain softening in nonviable trabeculae? (v) What changes occur in the dynamic (sinusoidal) stiffness and associated phase spectra, measured after axial muscle length extensions that demonstrate strain softening? It is our contention that only by finding unambiguous answers to these questions can we effect a 'bottom-up' approach to integrating data arising from healthy, isolated, cardiac tissue preparations into a sound understanding of diastolic mechanics.

Methods

All experiments were approved by the University of Auckland Animal Ethics Committee. Wistar rats (age 72 ± 34 days, weight 312 ± 76 g, means ± S.D.) were stunned and quickly killed by cervical dislocation. The thoracic cavity was opened and the heart, with approximately 10 mm of aorta, was quickly excised and plunged into a dish of 0°C dissection solution to induce arrest. The coronary circulation was immediately perfused with oxygen-saturated dissection solution using the Langendorff technique (Langendorff, 1895). Trabeculae, which were relatively long (2.15 ± 0.30 mm, $n = 14$) and sufficiently thin (178 ± 60 by 224 ± 100 μm) to ensure adequate oxygenation (Schouten & ter Keurs, 1986; Daut & Elzinga, 1988) were excised from the right ventricle. The trabeculae were mounted between a force transducer and an oscillatory motor, as described by Kirton *et al.* (2004). During mounting, care was taken not to stretch the muscle beyond resting (slack) length. Preparations were superfused at room temperature (20 ± 1°C) with dissection solution. The dissection solution was subsequently replaced with BDM-free solution and the muscle bath temperature increased to the standard experimental value of 26°C. The trabeculae were then stimulated until the twitch force was stable for at least 30 min.

The superfusate was a modified Tyrode solution (mM): NaCl, 141.6; KCl, 5.97; $MgCl_2$, 1; NaH_2PO_4, 1.18; Hepes, 10; glucose, 10; and $CaCl_2$, 0.5. The pH was adjusted to 7.4 using 1 M TRIS. The dissection solution was formed by addition of 20 mM BDM to the Tyrode solution. The preparations were superfused with the Tyrode solution in either the presence (+BDM, 50 mM) or absence of BDM (−BDM). Most solutions were vigorously bubbled with 100% O_2 (and are subsequently referred to as 'normoxic'), with the exception of those experiments in which hypoxia was induced, in which case the +BDM solutions were bubbled with 100% N_2. All chemicals were purchased from Sigma Aldrich and were of analytical grade.

The large-amplitude axial muscle extensions were supplied via a high-resolution linear actuator (M-227.25 DC-Mike, Physik Instrumente, Karlsbruhe, Germany), which was controlled via a 4-axis motor controller card (NI 7344, National Instruments, Austin, TX, USA). To determine the small-amplitude stiffness (dynamic stiffness) of the trabeculae, small-amplitude sinusoidal

length perturbations were applied via a piezoelectric actuator (Queensgate Technologies), which was located between the PI actuator and muscle attachment hook. The Queensgate actuator was controlled via a D–A channel from the data acquisition card. The lowest resonant frequency of the complete mechanical system was above 200 Hz.

Perturbations of muscle length (L_m) used to calculate dynamic stiffness were of small amplitude (~0.1% of L_m) and were sinusoidal at 33 frequencies between 0.2 and 100 Hz. The resulting oscillatory force changes (ΔF) were measured via the force transducer. To improve the signal-to-noise-ratio (SNR) of the measured force, a sinusoidal fitting technique was applied to both the measured change of muscle length (ΔL_m) and ΔF signals. The fitting algorithm constrained the fitted sinusoids to be the same frequency as the L_m perturbation signal and used a least-squares fit to an objective function:

$$\text{Objective function} = A_0 + A_1 \sin(\omega t) + A_2 \cos(\omega t). \quad (1)$$

This resulted in a single sine wave, offset by A_0 from zero, with magnitude

$$\text{Magnitude} = \sqrt{\left(A_1{}^2 + A_2{}^2\right)} \quad (2)$$

and phase

$$\text{Phase} = \arctan\left(\frac{A_2}{A_1}\right) = \phi. \quad (3)$$

This sinusoidal fitting technique reduces the effects of noise that is outside the frequency of perturbation and is the software equivalent of phase-lock-loop hardware, as employed by Wannenburg *et al.* (2000).

From the fitted data, the dynamic stiffness magnitude (henceforth 'stiffness') was determined as the dynamic ratio of stress to strain (units of gigapascals (GPa), comparable to Young's modulus). Dynamic stress was calculated as ΔF/trabeculae cross-sectional area at rest length, and the strain as $\Delta L_m/L_m$. The stiffness phase (henceforth 'phase'; eqn (3)) effectively measured the time interval between the peak magnitudes of ΔL_m and ΔF, divided by the period.

Sarcomere length (L_s) was set to ~1.9 μm at the beginning of each experiment, as described by Kirton *et al.* (2004). However, loss of contractile function, whether spontaneous or hypoxia induced, was often accompanied by a loss of regularity of sarcomere striation. Since determination of L_s depended on the clarity and contrast of striations, L_s could not be determined once viability had been lost.

Passive stress–L_m extension protocols

The mechanical perturbation protocol used to determine the stress (force per cross-sectional area at resting length) *versus* L_m relationship was similar to that used by Kirton *et al.* (2004). Briefly, experiments consisted of six stretch–release cycles (Cycles), which were of magnitude 5, 10 and 15% of muscle length (Stretch) and were repeated as appropriate (Sets). Electrical stimulation was stopped before each Set, following which BDM, if present, was washed out and trabecula viability tested by assessing the force response to electrical stimulation.

Use of resting cross-sectional area to calculate stress during muscle extension tends to underestimate the calculated stress, with underestimation being greatest at the largest extensions. For the dimensions of trabeculae used in this study, the underestimation of stress at 15% Stretch was calculated to be ~7%, assuming tissue incompressibility.

Strain softening was assessed by examining the stresses at a given L_m extension: (i) across Cycles at one level of Stretch; (ii) across Stretches within one Set; and (iii) across both Cycles and Stretches. Comparisons were made among: (i) viable trabeculae; (ii) those that had spontaneously become nonviable in oxygenated superfusate in either the presence ($+$BDM $+O_2$) or absence ($-$BDM $+O_2$) of BDM; and (iii) those rendered hypoxic in BDM ($+$BDM $-O_2$). Since recent studies performing mechanical testing of myocardium have been conducted with the tissue hypoxic in the presence of BDM (Emery *et al.* 1997; Dokos *et al.* 2002), and previous studies have shown that hypoxic trabeculae in the absence of BDM cease responding to electrical stimulation, develop contracture and display an increase of dynamic stiffness (Leijendekker *et al.* 1990; Bucx, 1993), it was deemed unnecessary to examine the behaviour of hypoxic trabeculae in the absence of BDM.

For most trabeculae that had spontaneously lost viability ($n = 11$) and all that were subjected to hypoxia ($n = 3$), the stress–L_m relationships were measured both before and after the loss of viability. Trabeculae that had spontaneously lost viability did so in both $+$BDM and $-$BDM solutions; those subjected to hypoxic intervention did so in $+$BDM solutions. For a small number of trabeculae, dynamic stiffness spectra were obtained both before and after the loss of viability, as well as after 5, 10 and 15% Stretches that demonstrated strain softening. All trabeculae were subjected to both $+$BDM $+O_2$ and $-$BDM $+O_2$ conditions.

Statistical analysis

Data were subjected to repeated measures ANOVAs appropriate for a $3 \times 3 \times 6$ (*Group* × *Stretch* × *Cycle*) design, where *Group* was the designation of environment (i.e. $+$BDM $+O_2$, $-$BDM $+O_2$, $+$BDM $-O_2$). Of particular interest in these analyses are the Group × Stretch and Stretch–Cycle interactions, significant results of which are reported. Differences among levels

of statistically significant ($P < 0.05$) main effects or interactions were sought, *post hoc*, using appropriate sets of mutually orthogonal contrast coefficients. All analyses were performed using SAS software. Unless otherwise stated, all data are presented as means ± S.E.M.

Results

Stress–L_m relationships in viable and nonviable trabeculae

Typical examples of the stress–L_m relationships recorded upon subjecting a quiescent trabecula, both when viable (Set 1) and when nonviable (Set 4), to 5 (black), 10 (dark grey) and 15% (light grey) Stretches are presented in Fig. 1. When recorded from viable trabeculae, the data for 5, 10 and 15% Stretches (Fig. 1*A*, Set 1) display an absence of irreversible strain softening. Upon loss of viability, the stress–L_m extension relationships change markedly (Fig. 1*B*). The relationships now display strain softening behaviour and are much stiffer for the same L_m extension compared with Fig. 1*A* (note difference in vertical scales). In approximately half the experiments, nonviable trabeculae buckled upon returning to resting position during a 15% Stretch. This behaviour was not observed in viable trabeculae, and indicated that the resting length of the nonviable trabeculae had become longer during the 15% L_m Stretch (i.e. the trabeculae had been irreversibly lengthened).

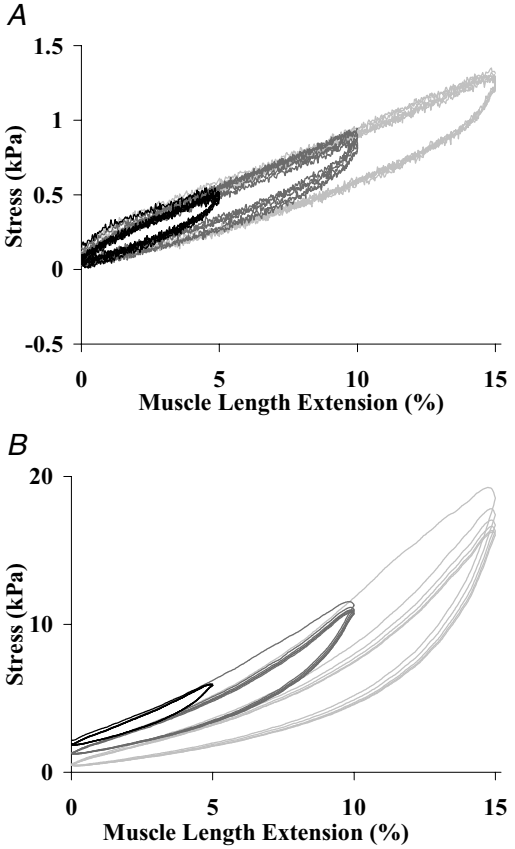

Figure 1. Typical stress–muscle length (L_m) extension relationships, measured during 6 Cycles of 5 (black line), 10 (dark grey line) and 15% L_m extensions (light grey line) at 25 μm s^{-1}
A, stress–L_m relationships during Set 1 of extensions, when the trabecula was viable (i.e. responding to electrical stimulation). Note that irreversible strain softening was not observed, since all the first extension curves followed the same stress–L_m extension curve. *B*, stress–L_m extension measured after the trabecula had become nonviable (i.e. ceased responding to electrical stimulation, Set 4). Note the increased stress scale, the presence of strain softening behaviour, the highly nonlinear stress–L_m extension relationships and the progressive loss of baseline tension *vis-à-vis A*.

Figure 2 demonstrates the stress–L_m extension relations for five Sets of 15% Stretch, all performed on the same trabecula. The trabecula was viable, and under normoxic, +BDM conditions during the first Set (S1, black), and hypoxic +BDM during the second to fifth Sets (S2, dark grey, through to S5, lightest grey). As the hypoxic period continued (S2 to S5), the slopes of the stress–L_m relationships increased, while strain softening behaviour progressively emerged (S2), steadily increasing in magnitude with time (S3 to S5). A small increase in baseline tension (contracture force) between S1 and S5 was also noted.

To test for strain softening, a similar statistical analysis to that performed by Kirton *et al.* (2004) was applied to the stress–L_m extension data obtained from nonviable trabeculae. The data used for this analysis were extracted from the Set in which the nonviable trabeculae appeared to have reached full stiffness. The data comprised the stress

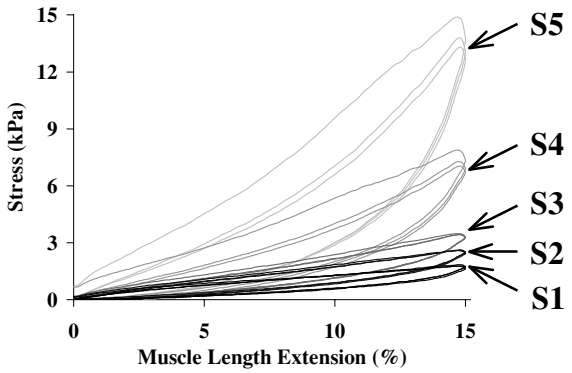

Figure 2. Stress–L_m extension relationships for 5 Sets of 15% Stretch
For clarity, only the first 3 of the 6 Cycles that were performed are shown. The first Set of 15% Stretches (S1, black) was performed when the trabecula was viable, normoxic and in BDM. The subsequent Sets of Stretches were performed while the trabecula was hypoxic and in BDM. The second Set (S2, very dark grey) through to the fifth Set (S5, lightest grey) show that the trabecula was progressively stiffening, with a small degree of strain softening first becoming evident during the 2nd Set (S2) and increasing in magnitude thereafter. The times from the start of the hypoxic intervention were 11, 22, 42 and 62 min for Sets 2, 3, 4 and 5, respectively.

measured at 3.5% L_m extension, from the six Cycles of 5, 10 and 15% Stretch, and the stress at 7% L_m extension, from the six Cycles of 10 and 15% Stretch.

Figure 3 summarizes the Cycle × Stretch interactions for both viable (Fig. 3*A* and *C*) and nonviable trabeculae (Fig. 3*B* and *D*), for stresses measured at 3.5 (Fig. 3*A* and *B*) and 7% L_m extensions (Fig. 3*C* and *D*). For the viable trabeculae ($n = 10$, Fig. 3*A* and *C*), a significant ($P < 0.001$) decrease of stress was demonstrated between Cycle 1 and Cycles 2–6. Since this stress loss recovered between Stretches and Sets, the decrease was attributed to reversible viscoelasticity. Conversely, strain softening was not detected in these viable trabeculae, since there was a lack of statistical difference between the stresses measured during the 5, 10 and 15% Stretches ($P > 0.13$ for 3.5% L_m extension and $P > 0.47$ for 7% L_m extension, Fig. 3*A* and *C*, respectively).

In contrast, the stresses for the nonviable trabeculae ($n = 14$), measured at 3.5 (Fig. 3*B*) and 7% L_m extension (Fig. 3*D*) showed significant strain softening behaviours. The statistical significance of the three main effects (i.e. Cycle, C1–C6; Extension, 3.5 and 7% L_m; and Stretch, 5, 10 and 15%), and all possible interactions, on stress ($n = 14$) was examined using repeated measures ANOVA. Both Cycle and Stretch demonstrated significant effects (in both cases $P < 0.0001$; see Table 1). For all Stretches of both 3.5 and 7% L_m extension, the first Cycle (C1) was stiffer than the remaining five Cycles. The five subsequent Cycles appeared to converge to a new, lower stiffness. There were significant differences of stress between 5, 10 and 15% Stretch (Fig. 3*B* and *D*, $P < 0.0001$). The softened stress measured for the last Cycle of a previous Stretch was the same as the stress for the first Cycle of a new larger Stretch. Therefore, strain softening, which by definition is irreversible, was detected in the nonviable trabeculae using the identical analysis that had found no strain softening in viable trabeculae.

Effect of BDM on compliance of nonviable trabeculae

The data for the nonviable trabeculae arose from three Groups: (i) normoxic trabeculae that had reached final stiffness in the presence of BDM (+BDM +O_2, $n = 8$); (ii) normoxic trabeculae that had reached final stiffness

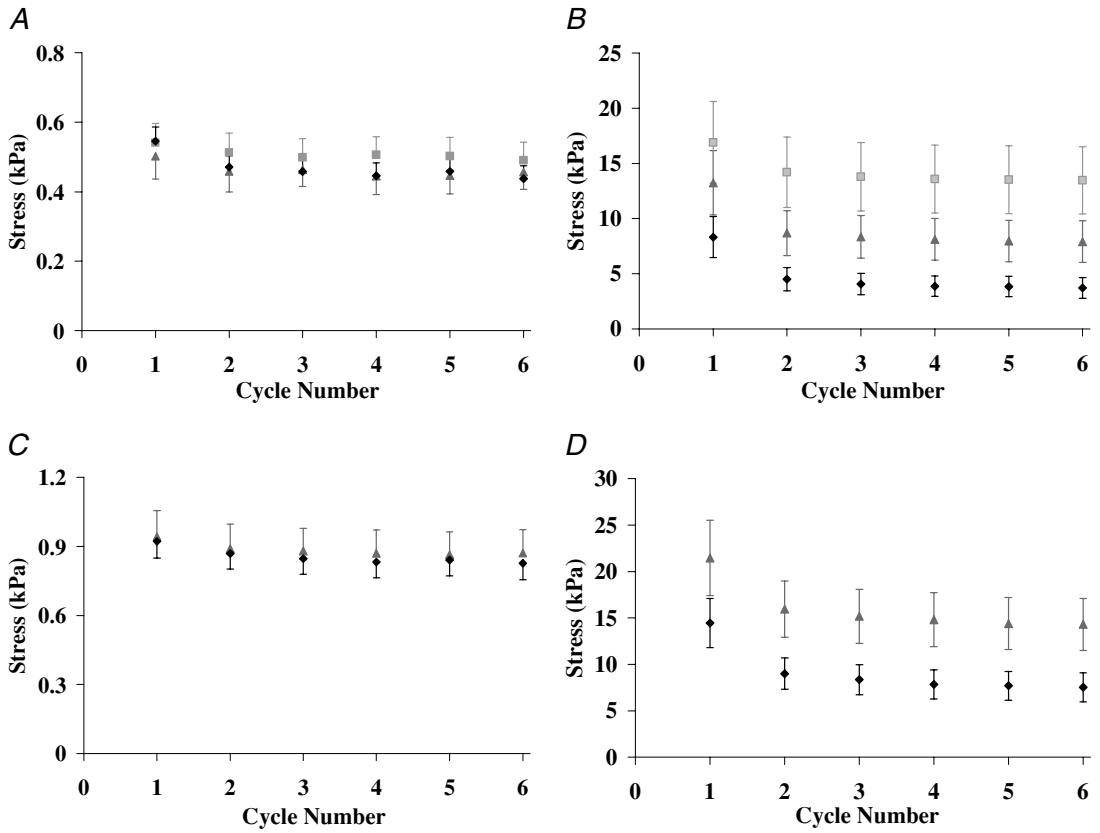

Figure 3. Average (± S.E.M.) stress per Cycle, measured during 5 (light grey squares), 10 (dark grey triangles) and 15% (black diamonds) Stretches of viable (*A* and *C*, $n = 10$) and nonviable (*B* and *D*, $n = 14$) trabeculae
A, stresses measured at 3.5% L_m extension for viable trabeculae. *B*, stresses measured at 3.5% L_m extension for nonviable trabeculae. *C*, stresses measured at 7% L_m extension for viable trabeculae. *D*, stresses measured at 7% L_m extension for nonviable trabeculae. Note differences in vertical scales.

Table 1. ANOVA-derived probabilities (*P* values) arising from tests of main effects and selected interactions on stress at 3.5 and 7% L_m, for electrically inexcitable trabeculae ($n = 14$)

	P value
Stretch	<0.0001
Extension	0.0001
Cycle	<0.0001
Group	0.058
Stretch × Extension	0.007
Stretch × Cycle	0.006
Extension × Cycle	0.007
Group × Stretch	0.063
Group × Extension	0.142
Group × Cycle	0.043

Note the statistically significant values of Stretch and Cycle, which indicate strain softening, and the nearly significant effect of Group, which suggests an effect of the perfusion environment in which the trabeculae stiffened.

in the absence of BDM ($-$BDM $+O_2$, $n = 3$); and (iii) hypoxic trabeculae that had stiffened in the presence of BDM ($+$BDM $-O_2$, $n = 3$).

Figure 4 compares the average (± S.E.M.) stresses for the three groups of nonviable trabeculae, as well as from viable trabeculae ($n = 10$), measured at 3.5% L_m extension during 15% Stretch. Of the nonviable trabeculae, $-$BDM $+O_2$ (triangles) were stiffest, $+$BDM $+O_2$ (squares) were less stiff and the hypoxic trabeculae ($+$ BDM $-O_2$, diamonds) were the most compliant. Viable trabeculae (crosses) were seen to be much more compliant than the nonviable trabeculae. ANOVA was used to examine the statistical significance of Group on stress (See Table 1; note that data from viable trabeculae were not included). While there appeared to be differences among these Groups, application of ANOVA showed the differences to be nonsignificant ($P = 0.058$). The data for each Group were analysed separately with strain softening being observed in each Group, as seen by significant effects of both Stretch and Cycle on stress ($+$BDM $+O_2$, $n = 8$, $P = 0.004$, $P < 0.0001$; $-$BDM $+O_2$: $n = 3$, $P = 0.028$, $P = 0.0001$; and $+$BDM $-O_2$, $n = 3$, $P = 0.0029$, $P < 0.0001$, respectively). Therefore, the presence of BDM did not prevent the appearance of strain softening in these nonviable specimens.

Dynamic stiffness of viable and nonviable trabeculae

Typical dynamic stiffness and phase spectra for cardiac trabeculae, when viable (quiescent state, crosses), activated (Ba^{2+}-induced contracture, light grey squares) and nonviable (rigor state, dark grey circles), are found in Fig. 5. The stiffness of a trabecula when quiescent (black) and in rigor (light grey) increased with frequency (Fig. 5*A*). Note, in this instance, that the trabecula was ~7 times stiffer in rigor than when quiescent. In contrast, the Ba^{2+}-activated muscle displayed a much more complicated stiffness spectrum. The stiffness was low at low frequencies and high at high frequencies, with the transition between low and high stiffness occurring over a narrow frequency range. The phase relationships displayed similar trends. The quiescent or rigor muscle displayed near linear and slightly positive phase spectra that superimposed, while the activated muscle displayed a much more complicated phase spectrum (Fig. 5*B*).

Dynamic stiffness measurements were made on three trabeculae, both when viable and when nonviable, before any stretches had been applied and again after 5, 10 and 15% Stretches that elicited strain softening (Fig. 6*A*). These trabeculae did not display buckling behaviour during release from 15% stretch. After a viable trabecula (black dotted line) had become nonviable (black continuous line), the dynamic stiffness increased uniformly across all measured frequencies. After 5 (dark grey), 10 (grey dotted) and 15% (light grey) Stretches, the dynamic stiffness decreased uniformly across all measured frequencies. Note that the phase spectra were almost unchanged during the stiffening or strain softening process (Fig. 6*B*). A linear relationship was found between the contracture tension (at zero L_m extension) and the stiffness at 100 Hz (nondimensional slope of 67 ± 6, $n = 3$, data not presented) measured at full rigor and after 5, 10 and 15% Stretch that exhibited strain softening.

Discussion

Strain softening behaviour, which is absent in intact, viable, rat RV trabeculae (see Fig. 1*A* and Kirton *et al.* 2004), becomes readily apparent (Fig. 1*B*) once trabeculae lose viability (defined as unresponsiveness to electrical stimulation). It has previously been shown that strain softening is absent whether or not BDM is present (Kirton *et al.* 2004). The present study demonstrates that strain softening appears in both hypoxic and spontaneously nonviable trabeculae, in both the presence and absence of BDM (Fig. 3).

The spontaneous loss of viability was manifested by a lack of response to electrical stimulation and was accompanied by loss of visible striations, increased slope of the stress–L_m extension relationship, and uniform increase in dynamic stiffness across all frequencies between 0.2 and 100 Hz (Fig. 6*A*). A gradual increase in baseline tension was also noted (Fig. 2), which was more pronounced in the absence of BDM. It was observed that trabeculae that were prone to losing viability during the course of an experiment usually exhibited an elevated level of spontaneous activity (writhing) during dissection and mounting, even when the bath temperature was increased to 26°C (see also de Tombe & ter Keurs, 1990). This behaviour is commonly attributed to intracellular calcium overload in response to tissue damage suffered during dissection or mounting. It is

well known that elevated $[Ca^{2+}]_i$ leads to calcium-induced calcium release and ultimately, if $[Ca^{2+}]_i$ remains high, to depletion of ATP and cardiac hypercontracture (Hoerter *et al.* 1986). Thus, it is not surprising that specimens which display excessive spontaneous activity become electrically nonresponsive and ultimately stiffen.

Possible causes of strain softening behaviour

Since strain softening has been reported in a variety of cardiac preparations and there are many potential causes. In the following sections we consider architectural, mechanical and metabolic possibilities.

Over-extension. Strain softening has been reported during both physiological and supraphysiological levels of strain in intact cardiac tissue (Emery *et al.* 1997, 1998; Dokos *et al.* 2002). Emery *et al.* (1998) produced micrographic evidence of damaged perimysial fibres in hearts that had been inflated to 120 mmHg, and described this as 'over-inflation damage'. Strain softening has also been reported during axial extensions of skinned cardiac myocytes (Granzier & Irving, 1995) and individual cardiac myofibrils (Linke *et al.* 1994; Linke *et al.* 1996), although only at L_s extensions greater than 3 μm. For L_s extensions less than 2.3 μm, titin displayed viscoelastic softening, which fully recovered after 10 s of rest (Helmes *et al.* 1999; Kellermayer *et al.* 2001). When intact rat cardiac trabeculae are axially extended, the maximum extension of sarcomere length, above which the viability of the specimen is compromised, has been reported to be 2.3 μm (de Tombe & ter Keurs, 1992; Hanley *et al.* 1999).

We have previously shown (Kirton *et al.* 2004) that viable trabeculae do not exhibit strain softening for L_s extensions of up to 2.3 μm when due care is taken to avoid extending the samples before and during mounting. The present study has demonstrated the appearance of strain softening for comparable L_m extensions when viability is lost (Fig. 1). We conclude that, while over-extension may be a *sufficient*, it is not a *necessary*, contributor to strain softening.

Cutting injury. Dokos *et al.* (2002) and Humphrey *et al.* (1990) both used tissue that had been excised from the heart wall. It is difficult to imagine that cut edges would not sustain some injury. Such cutting injury may explain the unexpectedly low compliance in the fibre direction during biaxial testing of isolated canine myocardium (Demer & Yin, 1983) as well as during shear deformation of blocks of pig myocardium (Dokos *et al.* 2002). It is noteworthy

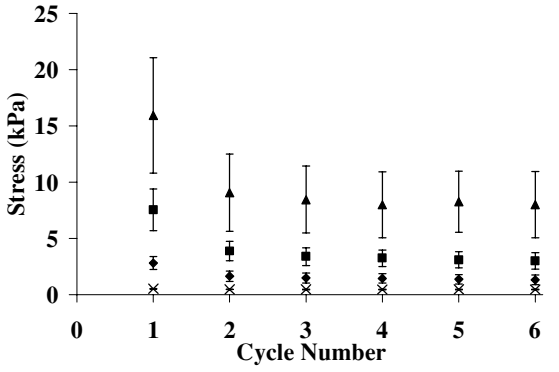

Figure 4. Mean (± S.E.M.) stress per Cycle as measured at 3.5% L_m extension for 6 Cycles of 15% Stretch
Stress data for nonviable trabeculae arose from 3 experimental interventions: normoxic +BDM (squares, $n = 8$), normoxic −BDM (triangles, $n = 3$) and hypoxic +BDM (diamonds, $n = 3$). Comparable stress data for viable trabeculae (from Kirton *et al.* 2004) are also included (crosses, $n = 10$); error bars smaller than symbols.

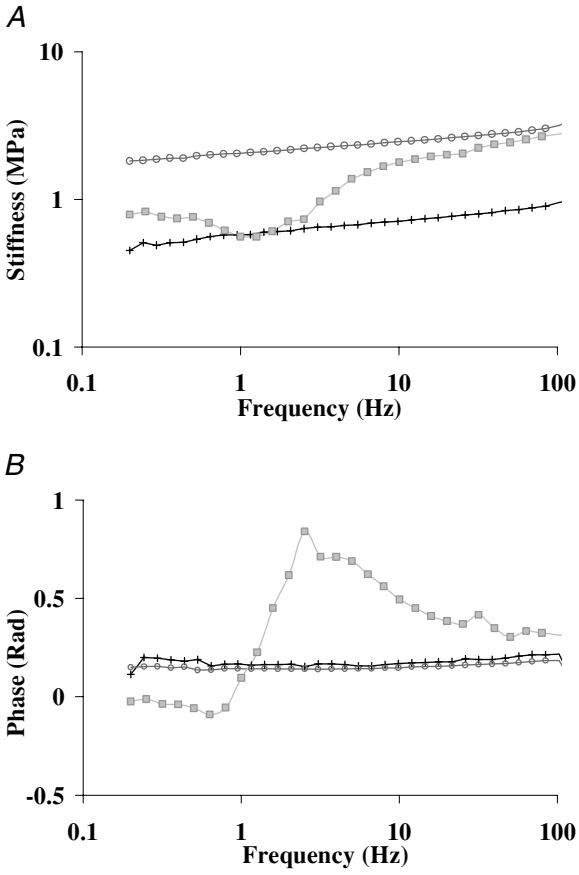

Figure 5. Typical stiffness (*A*) and phase (*B*) spectra of a trabecula when quiescent (black line and crosses), Ba^{2+} activated (light grey line and black squares) and in rigor (dark grey line and circles)
When trabeculae were quiescent (viable) or in rigor (nonviable), both the stiffness and phase spectra had a linear dependence on the logarithm of frequency, although the stiffness was ~7-fold greater in rigor than in quiescence. When trabeculae were Ba^{2+} activated, both the stiffness and phase relationships became much more complex. Note that the spectra for Ba^{2+} activation were acquired from a different trabecula from those of the quiescent and rigor spectra.

that the strain softening observed by Dokos *et al.* (2002) occurred in the presence of BDM.

BDM. Butanedione monoxime is considered to be cardioprotective, since it protects cardiac tissue from cutting damage (Mulieri *et al.* 1989), the calcium paradox (Daly *et al.* 1987) and reperfusion injury (Nayler *et al.* 1988). It also inhibits contractile function (see review by Sellin & McArdle, 1994) and has been reported to lower, or to have no effect on, ATP consumption (Armstrong & Ganote, 1991; Allen *et al.* 1998).

In contrast with these beneficial properties, BDM has been reported to cause tissue damage. At 37°C, 50 mM BDM was observed to accelerate contracture and the rate of ATP depletion in intact rat cardiomyocytes poisoned with cyanide (Stapleton *et al.* 1998). While the presence of 20 mM BDM was reported to inhibit contracture of rat cardiomyocytes during anoxia, it was nevertheless associated with accelerated cell injury, as measured by release of myoglobin and ultrastructural defects in the sarcolemmal membrane (Armstrong & Ganote, 1991). The 'energy cost per unit force' of cardiac muscles was reported to increase in the presence of BDM in a dose-dependent manner, whereas in skeletal muscle no corresponding effect was observed (Ebus & Stienen, 1996).

We have previously reported that viable trabeculae show no evidence of strain softening, whether or not BDM is present (Kirton *et al.* 2004). In the present study, nonviable trabeculae demonstrated strain softening in both the presence and absence of BDM (Fig. 4). From these results we conclude that BDM neither induces nor prevents strain softening behaviour in cardiac tissue.

While BDM could neither prevent nor abolish strain softening in nonviable trabeculae, and had a statistically nonsignificant ($P = 0.058$) effect on tissue compliance, it nevertheless appeared to reduce the measured stiffness (Fig. 4). Trabeculae that spontaneously stiffened in the absence of BDM were somewhat stiffer, and displayed more strain softening, than those stiffening in the presence of BDM. This observation is consistent with reports in the literature, which show that time-to-contracture is significantly increased by the presence of BDM in metabolically challenged cardiac tissue (Hajjar *et al.* 1994; Ikenouchi *et al.* 1994). Concurrently, a lower final rigor force was reported when BDM was added before rigor was induced in both metabolically challenged rat myocytes (Stapleton *et al.* 1998) and skinned skeletal muscle (Fryer *et al.* 1988). Thus, trabeculae that had stiffened in the absence of BDM would have reached their final contracture state faster and probably with cross-bridges in a conformation exhibiting higher stiffness.

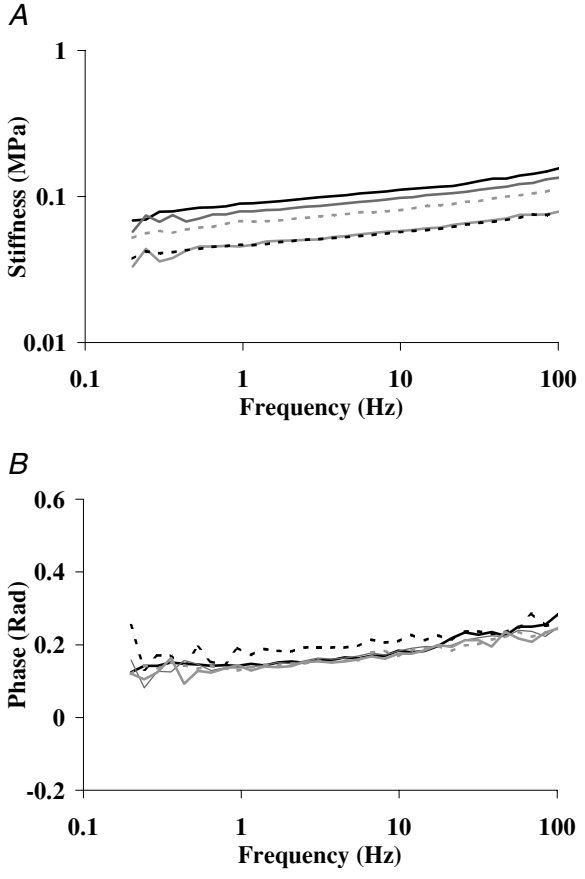

Figure 6. Typical changes in the linear stiffness–frequency (*A*) and phase–frequency (*B*) spectra of a quiescent trabecula, when viable (black dashed line) and when subsequently fully stiffened and nonviable (black continuous line)
Once nonviable, the dynamic stiffness of the trabecula was measured after 5, 10 and 15% Stretches, during which strain softening behaviour was demonstrated (5%, dark grey continuous line; 10%, light grey dashed line; and 15%, light grey continuous line).

Tissue ill-health. Viable trabeculae that initially show no evidence of strain softening exhibit strain softening behaviour upon becoming nonviable (Fig. 1). Concurrent with the emergence of strain softening behaviour there is an increase in both the slope and the extent of hysteresis of the stress–L_m relationship (Fig. 2), and a uniform increase in stiffness at all frequencies with no associated change of phase (Fig. 6). The emergence of strain softening occurs whether loss of viability arises spontaneously or is experimentally induced through hypoxia (Fig. 4). The magnitude of strain softening, the slope of the stress–L_m extension relationship and, to a lesser degree, baseline tension, each increase with time (Fig. 2, curves S2–S5). It should be noted that the stress–L_m extension relationships for Stretches S2, S3 and S4 (Fig. 2) did not display classical irreversible strain softening, since the preparation was continuing to stiffen while these measurements were being made. The results did, however, show relatively long-lasting (~5 min) strain softening behaviour. Hence, this softening was unlike the reversible viscoelastic behaviour that characterizes both viable

trabeculae (Kirton *et al.* 2004) and titin preparations (Helmes *et al.* 1999).

Increased slope of a stress–L_m relationship upon spontaneous loss of viability can be attributed to the formation of rigor cross-bridges, as opposed to an increase in asynchronous cross-bridge cycling associated with increased intracellular calcium. This inference is based on the large, uniform increase of dynamic stiffness at all measured frequencies, in conjunction with the lack of effect on the phase response (Fig. 6; Leijendekker *et al.* 1990; Bucx, 1993). The linear stiffness and phase spectra shown in Fig. 6 are comparable to those measured in quiescent and rigor muscle and contrast with the more complex spectra observed when Ba^{2+}-activated cross-bridges are cycling (Fig. 5). Such a uniform increase in dynamic stiffness, with associated flat phase response, is routinely reported for tissues in rigor (Kawai & Brandt, 1980; Saeki *et al.* 1991; Campbell *et al.* 1993; Hajjar *et al.* 1994). The observed complex spectra demonstrated with Ba^{2+} have frequently been reported for Ba^{2+}- and Ca^{2+}-activated skeletal muscle (Kawai & Brandt, 1980), as well as for cardiac preparations, such as the left ventricular chamber (Campbell *et al.* 1993), papillary muscles (Saeki *et al.* 1978, 1991; Rossmanith, 1986; Campbell *et al.* 1993; Hajjar *et al.* 1994) and cardiac trabeculae (Rossmanith *et al.* 1986; Leijendekker *et al.* 1990; Saeki *et al.* 1991; Bucx, 1993). In the present study, hypoxic trabeculae exhibited an increased slope of the stress–L_m extension relationships and rigor-like increases in dynamic stiffness behaviour, which were similar to the behaviour observed in trabeculae that had become spontaneously nonviable.

The two principal mechanisms proposed for hypoxia-induced contracture are rigor cross-bridge formation, due to ATP depletion, and an increase in the number of cycling cross-bridges, due to an increase in intracellular Ca^{2+} concentration (Haworth *et al.* 1988; Koretsune & Marban, 1990). Koretsune & Marban (1990) studied ischaemic contracture in rabbit hearts and found that contracture closely coincided with depletion of [ATP] to below 10% of control levels, but not with the elevation of $[Ca^{2+}]_i$. Complementing these findings were studies of isolated rat cardiac myocytes reporting that cells enter hypoxic contracture when [ATP] is depleted below 10% of control values (Stern *et al.* 1985; Haworth *et al.* 1988). Two studies investigating hypoxic interventions in rat cardiac trabeculae reported that the increase in stiffness (at 1 and 100 Hz) is solely attributable to formation of rigor cross-bridges (i.e. to ATP depletion) and not to Ca^{2+}-activated cross-bridges (Leijendekker *et al.* 1990; Bucx, 1993). Interestingly, measurable levels of rigor cross-bridge formation were reported within 2–3 min of hypoxia, whereas contracture force did not start to increase for 5 min in trabeculae responding to 1 Hz stimulation (Leijendekker *et al.* 1990). From these studies it appears that hypoxic contracture is induced by rigor cross-bridge formation subsequent to ATP depletion.

When rat trabeculae are subjected to no-flow hypoxia (30°C, 1 Hz stimulation), active force decreases almost instantaneously (Bucx, 1993). Likewise, when ferret whole hearts are subjected to ischaemia (30°C, 1.2 Hz stimulation), active force is attenuated by ∼85% in much less than 1 min (Koretsune & Marban, 1990). As the following considerations show, the energy demands of such hypoxic preparations may be rather high. The basal metabolic rate of rat myocardium is some 30–35% of total cardiac metabolism (Gibbs & Loiselle, 2001). While no reduction of basal metabolism of guinea-pig trabecula was detectable when using 10 mM BDM (Schramm *et al.* 1994), a 20% reduction was observed when using rat left ventricular slices (Yasuhara *et al.* 1996). If we apply the latter value as a 'correction', we see that the metabolic rate of quiescent, BDM-arrested, ischaemic cardiac tissue may remain as high as ∼25% of total active metabolism. Under this scenario, ischaemic, BDM-arrested, quiescent heart preparations would still have significant energy requirements, and anoxia would ensue in less than 1 min.

Both Leijendekker *et al.* (1990) and Bucx (1993) reported an increase in stiffness (at 1 and 100 Hz) that was linearly proportional to the increase in contracture tension. Since the increase in stiffness at 1 and 100 Hz is detectable during very small (1%) L_m oscillations, it has been attributed to the formation of rigor cross-bridges (Leijendekker *et al.* 1990; Bucx, 1993). The present study shows that, once strain softening is observed, loss of stiffness is uniform across the frequency spectrum (Fig. 6). This is consistent with the hypothesis that strain softening reflects irreversible damage to passive (i.e. nonactively cycling) structural elements within tissue that is in a state of partial, or full, rigor.

Both Stern *et al.* (1985) and Haworth *et al.* (1988) reported large variability in the time to hypoxia-induced contracture of cardiomyocytes, although the shortening event itself occurred in less than 10 s. From their results both groups of investigators speculated that isolated cardiac myocytes have variable [ATP], which suggests that cardiac myocytes in multicellular and whole-heart preparations may also have variable [ATP]. If this is correct, then when they are metabolically challenged through ischaemia or hypoxia, some myocytes could be depleted of ATP and form rigor cross-bridges, while adjacent cells could remain fully viable and capable of producing active force (Leijendekker *et al.* 1990). Such a putative heterogeneous mixture of healthy and rigor cells would promote a gradual increase in contracture force and stiffness, while active force would slowly decrease. Exactly such behaviour has been reported in hypoxic trabeculae (Leijendekker *et al.* 1990; Bucx, 1993) as well as in metabolically inhibited papillary muscle (Hajjar *et al.* 1994). Furthermore, Stern *et al.* (1985) reported

that cardiac myocytes that had experienced hypoxic contracture for less than 10 min recovered some degree of contractile function, whereas those that had undergone hypoxic contracture for more than 20 min underwent hypercontracture upon re-introduction of oxygen. Taken together, these results suggest that caution is necessary when using partial recovery of contractile function as evidence that previously hypoxic or ischaemic specimens are free of rigor cross-bridges.

Further studies have reported large degrees of spatial heterogeneity of physiological parameters between adjacent sites within the left ventricular wall of whole hearts. Such variability within the left ventricular wall has been demonstrated for perfusion (as measured using either the microsphere technique, Prinzen & Bassingthwaighte, 2000; Laussmann *et al.* 2002, or high-resolution MRI, Bauer *et al.* 2001), glucose uptake (Deussen, 1997), energy turnover (Decking *et al.* 2001), energy demand (Loncar *et al.* 1998) and protein expression (Laussmann *et al.* 2002). Indeed, one study found spatially heterogeneous impairment of myocyte viability during partial coronary occlusion (Brasch *et al.* 1999), which indicates that local energy demand, too, is inhomogeneous within the left myocardial wall.

From these various results we draw the following inferences: adjacent myocytes can have different energy requirements; myocytes with higher energy requirements are more susceptible to ischaemic or hypoxic injury; and during hypoxia myocytes have a large variation in time-to-contracture. These inferences suggest that, during a hypoxic insult, rigor cells occur adjacent to healthy contractile cells. This explains why, during hypoxic intervals, a small but measurable number of rigor cross-bridges form within 2 min, increasing thereafter (Leijendekker *et al.* 1990). This hypothesis predicts that the number of cells in rigor increases with time at the expense of viable cells, and explains why contracture force increases while active force decreases during hypoxic interventions (Koretsune & Marban, 1990; Leijendekker *et al.* 1990; Bucx, 1993; Hajjar *et al.* 1994). An alternative, but unlikely, hypothesis is that within each cell a small number of rigor cross-bridges exist alongside cycling cross-bridges. This would require large spatial gradients of [ATP] within a cell. Our hypothesis, that a heterogeneous mixture of rigor and healthy cells exists throughout a hypoxic multicellular preparation, explains the appearance of strain softening and the initially slow increase in the slope of the stress–L_m relation (Fig. 2). The 11 min rest intervals between the Sets of Stretches allowed previously healthy cells progressively to enter rigor, with the result that the magnitude of strain softening increased with time (Fig. 2).

Our hypothesis also accommodates, without recourse to differences in tissue architecture, the disparate results of Emery (1997) and Emery *et al.* (1998). His finding, of a 2-fold greater extent of strain softening in the fibre direction than in the cross-fibre or fibre-shear direction, supports our hypothesis that strain softening is the result of irreversible, strain-induced damage to tissue in rigor. Furthermore, the absence of strain softening in viable superfused mouse papillary muscles, despite its presence in nonperfused mouse whole-heart preparations, can also be explained by our tissue viability hypothesis. That is, strain softening was not observed in tissues that were viable, while it was observed in tissue whose viability was not assessed.

Conclusions

When subjected to axial length extensions, trabeculae exhibit strain softening behaviour upon becoming electrically nonresponsive. The stress–L_m extension relationships of trabeculae become much steeper when the preparations lose viability. The appearance of strain softening is independent of the presence of BDM. Dynamic stiffness increases uniformly across all frequencies upon loss of viability. This observation has been linked to rigor cross-bridge formation, which has been reported to occur within a short time (2 min) during hypoxic interventions (Leijendekker *et al.* 1990). When strain softening is observed during muscle length extensions, dynamic stiffness decreases uniformly at all frequencies. The results of the present study support reports in the literature suggesting that hypoxic and ischaemic cardiac tissues contain a heterogeneous mixture of rigor and healthy cells.

Given that our long-term objective, in general, is to integrate the behaviour of isolated cardiac preparations into models of the whole heart and, in particular, to describe the mechanical behaviour of the diastolic heart, care must be taken to account for possible artefacts in the experimental methodology. Experiments that assess the passive material properties of myocardial tissue should also assess the responsiveness of the tissue to electrical stimulation.

References

Allen TJA, Mikala G, Wu X-P & Dolphin AC (1998). Effects of 2,3-butanedione monoxime (BDM) on calcium channels expressed in *Xenopus* oocytes. *J Physiol* **50**, 1–14.

Armstrong SC & Ganote CE (1991). Effects of 2,3-butanedione monoxime (BDM) on contracture and injury of isolated rat myocytes following metabolic inhibition and ischemia. *J Mol Cellular Cardiol* **23**, 1001–1014.

Bauer WR, Hiller KH, Galuppo P, Neubauer S, Kopke J, Haase A, Waller C & Ertl G (2001). Fast high-resolution magnetic resonance imaging demonstrates fractality of myocardial perfusion in microscopic dimensions. *Circulation Res* **88**, 340–346.

Brasch F, Neckel M, Volkmann R, Schmidt G, Hellige G & Vetterlein F (1999). Mapping of capillary flow, cellular redox state, and resting membrane potential in hypoperfused rat myocardium. *Am J Physiol* **277**, H2050–H2064.

Bucx JJ (1993). Ischemia of the heart; a study of sarcomere dynamics and cellular metabolism. PhD Thesis, University of Calgary, Calgary.

Campbell KB, Taheri H, Kirkpatrick RD, Burton T & Hunter WC (1993). Similarities between dynamic elastance of left ventricular chamber and papillary muscle of rabbit heart. *Am J Physiol* **264**, H1926–H1941.

Daly MJ, Elz JS & Nayler WG (1987). Contracture and the calcium paradox in the rat heart. *Circulation Res* **61**, 560–569.

Daut J & Elzinga G (1988). Heat production of quiescent ventricular trabeculae isolated from guinea-pig heart. *J Physiol* **398**, 259–275.

Decking UK, Skwirba S, Zimmermann MF, Preckel B, Thamer V, Deussen A & Schrader J (2001). Spatial heterogeneity of energy turnover in the heart. *Pflügers Arch* **441**, 663–673.

Demer LL & Yin FC (1983). Passive biaxial mechanical properties of isolated canine myocardium. *J Physiol* **339**, 615–630.

de Tombe PP & ter Keurs HE (1990). Force and velocity of sarcomere shortening in trabeculae from rat heart. *Circulation Res* **66**, 1239–1254.

de Tombe PP & ter Keurs HE (1992). An internal viscous element limits unloaded velocity of sarcomere shortening in rat myocardium. *J Physiol* **454**, 619–642.

Deussen A (1997). Local myocardial glucose uptake is proportional to, but not dependent on blood flow. *Pflügers Arch* **433**, 488–496.

Dokos S, Smaill BH, Young AA & LeGrice IJ (2002). Shear properties of passive ventricular myocardium. *Am J Physiol* **283**, H2650–H2659.

Ebus JP & Stienen GJM (1996). Effects of 2,3-butanedione monoxime on cross-bridge kinetics in rat cardiac muscle. *Pflugers Arch* **432**, 921–929.

Emery JL (1997). Load-history dependence of resting ventricular myocardium. PhD Thesis, University of California, San Diego, CA, USA.

Emery JL, Omens JH, Mathieu-Costello OA & McCulloch AD (1998). Structural mechanisms of acute ventricular strain softening. *Int J Cardiovascular Med Science* **1**, 241–250.

Emery JL, Omens JH & McCulloch AD (1997). Strain softening in rat left ventricular myocardium. *J Biomechan Engineering* **119**, 6–12.

Fiegl EO (1983). Coronary physiology. *Phyiol Rev* **63**, 1–205.

Fryer MW, Neering IR & Stephenson DG (1988). Effects of 2,3-butanedione monoxime on the contractile activation properties of fast- and slow-twitch rat muscle fibres. *J Physiol* **407**, 53–75.

Gibbs CL & Loiselle DS (2001). Cardiac basal metabolism. *Jap J Physiol* **51**, 399–426.

Granzier HL & Irving TC (1995). Passive tension in cardiac muscle: contribution of collagen, titin, microtubules, and intermediate filaments. *Biophys J* **68**, 1027–1044.

Gutierrez C & Blanchard DG (2004). Diastolic heart failure: challenges of diagnosis and treatment. *Am Family Physician* **69**, 2609–2616.

Hajjar RJ, Ingwall JS & Gwathmey JK (1994). Mechanism of action of 2,3-butanedione monoxime on contracture during metabolic inhibition. *Am J Physiol* **267**, H100–H108.

Hanley PJ, Young AA, LeGrice IJ, Edgar SG & Loiselle DS (1999). 3-Dimensional configuration of perimysial collagen fibres in rat cardiac muscle at resting and extended sarcomere lengths. *J Physiol* **517**, 831–837.

Haworth RA, Nicolaus A, Goknur AB & Berkoff HA (1988). Synchronous depletion of ATP in isolated adult rat heart cells. *J Mol Cellular Cardiol* **20**, 837–846.

Helmes M, Trombitas K, Centner T, Kellermayer M, Labeit S, Linke WA & Granzier H (1999). Mechanically driven contour-length adjustment in rat cardiac titin's unique N2B sequence: titin is an adjustable spring. *Circulation Res* **84**, 1339–1352.

Hoerter JA, Miceli MV, Renlund DG, Jacobus WE, Gerstenblith G & Lakatta EG (1986). A phosphorus-31 nuclear magnetic resonance study of the metabolic, contractile, and ionic consequences of induced calcium alterations in the isovolumic rat heart. *Circulation Res* **58**, 539–551.

Humphrey JD, Strumpf RK & Yin FC (1990). Determination of a constitutive relation for passive myocardium: I. A new functional form. *J Biomechan Engineering* **112**, 333–339.

Ikenouchi H, Zhao L & Barry WH (1994). Effect of 2,3-butanedione monoxime on myocyte resting force during prolonged metabolic inhibition. *Am J Physiol* **267**, H419–H430.

Kawai M & Brandt PW (1980). Sinusoidal analysis: a high resolution method for correlating biochemical reactions with physiological processes in activated skeletal muscles of rabbit, frog and crayfish. *J Muscle Res Cell Motility* **1**, 279–303.

Kellermayer MS, Smith SB, Bustamante C & Granzier HL (2001). Mechanical fatigue in repetitively stretched single molecules of titin. *Biophys J* **80**, 852–863.

Kirton RS, Taberner AJ, Young AA, Nielsen P & Loiselle DS (2004). Strain-softening is not present during axial extensions of rat intact right-ventricular trabeculae, in the presence or absence of 2,3-butanedione monoxime. *Am J Physiol* **286**, H708–H715.

Koretsune Y & Marban E (1990). Mechanism of ischemic contracture in ferret hearts: relative roles of $[Ca^{2+}]_i$ elevation and ATP depletion. *Am J Physiol* **258**, H9–H16.

Langendorff O (1895). Untersuchungen am überlebenden Säugethierherzen. *Arch die Gesamte Physiologie* **61**, 291–332.

Laussmann T, Janosi RA, Fingas CD, Schlieper GR, Schlack W, Schrader J & Decking UK (2002). Myocardial proteome analysis reveals reduced NOS inhibition and enhanced glycolytic capacity in areas of low local blood flow. *FASEB J* **16**, 628–630.

Leijendekker WJ, Gao WD & ter Keurs HE (1990). Unstimulated force during hypoxia of rat cardiac muscle: stiffness and calcium dependence. *Am J Physiol* **258**, H861–H869.

Linke WA, Bartoo ML, Ivemeyer M & Pollack GH (1996). Limits of titin extension in single cardiac myofibrils. *J Muscle Res Cell Motility* **17**, 425–438.

Linke WA, Popov VI & Pollack GH (1994). Passive and active tension in single cardiac myofibrils. *Biophys J* **67**, 782–792.

Loncar R, Flesche CW & Deussen A (1998). Coronary reserve of high- and low-flow regions in the dog heart left ventricle. *Circulation* **98**, 262–270.

McCulloch AD, Hunter PJ & Smaill BH (1992). Mechanical effects of coronary perfusion in the passive canine left ventricle. *Am J Physiol* **262**, H523–H530.

Mulieri LA, Hasenfuss G, Ittleman F, Blanchard EM & Alpert NR (1989). Protection of human left ventricular myocardium from cutting injury with 2,3-butanedione monoxime. *Circulation Res* **65**, 1441–1449.

Nayler WG, Elz JS & Buckley DJ (1988). The stunned myocardium: effect of electrical and mechanical arrest and osmolarity. *Am J Physiol* **255**, H60–H69.

Prinzen FW & Bassingthwaighte JB (2000). Blood flow distributions by microsphere deposition methods. *Cardiovascular Res* **45**, 13–21.

Rossmanith GH (1986). Tension responses of muscle to *n*-step pseudo-random length reversals: a frequency domain representation. *J Muscle Res Cell Motility* **7**, 299–306.

Rossmanith GH, Hoh JFY, Kirman A & Kwan LJ (1986). Influence of V_1 and V_3 isomyosins on the mechanical behaviour of rat papillary muscle as studied by pseudo-random binary noise modulated length perturbations. *J Muscle Res Cell Motility* **7**, 307–319.

Saeki Y, Kawai M & Zhao Y (1991). Comparison of crossbridge dynamics between intact and skinned myocardium from ferret right ventricles. *Circulation Res* **68**, 772–781.

Saeki Y, Sagawa K & Suga H (1978). Dynamic stiffness of cat heart muscle in Ba^{2+}-induced contracture. *Circulation Res* **42**, 324–333.

Schouten VJA & ter Keurs HE (1986). The force-frequency relationship in rat myocardium: the influence of muscle dimensions. *Pflugers Arch* **407**, 14–17.

Schramm M, Klieber H-G & Daut J (1994). The energy expenditure of actomyosin-ATPase, Ca^{2+}-ATPase and Na^+,K^+-ATPase in guinea-pig cardiac ventricular muscle. *J Physiol* **481**, 647–662.

Sellin LC & McArdle JJ (1994). Multiple effects of 2,3-butanedione monoxime. *Pharmacol Toxicol* **74**, 305–313.

Stapleton MT, Fuchsbauer CM & Allshire AP (1998). BDM drives protein dephosphorylation and inhibits adenine nucleotide exchange in cardiomyocytes. *Am J Physiol* **275**, H1260–H1266.

Stern MD, Chien AM, Capogrossi MC, Pelto DJ & Lakatta EG (1985). Direct observation of the 'oxygen paradox' in single rat ventricular myocytes. *Circulation Res* **56**, 899–903.

Wannenburg T, Heijne GH, Geerdink JH, Van Den Dool HW, Janssen PM & de Tombe PP (2000). Cross-bridge kinetics in rat myocardium: effect of sarcomere length and calcium activation. *Am J Physiol* **279**, H779–H790.

Yasuhara S, Takaki M, Kikuta A, Ito H & Suga H (1996). Myocardial $\dot{V}_{O_2}$ of mechanically unloaded contraction of rat ventricular slices measured by a new approach. *Am J Physiol* **270**, H1063–H1070.

Acknowledgements

We acknowledge the generous financial support of the Royal Society of New Zealand (Marsden Fund), the New Zealand Foundation for Research, Science & Technology (FRST) and the Health Research Council of New Zealand.